

A Differentiable Framework for Global Circulation Model Precipitation Bias Correction

Kamlesh Sawadekar, Seth McGinnis, Peijun Li, Chaopeng Shen*

* Corresponding author. cshen@engr.psu.edu

Abstract

Systematic biases in Global Circulation Model (GCM) outputs limit their direct applicability in regional planning, necessitating bias correction. Correcting precipitation is particularly challenging due to its non-Gaussian distribution, intermittent nature, and non-linear extremes. However, traditional statistical methods cannot learn from big data and easily address systematic biases in GCMs, and while machine learning does provide this flexibility, their black-box type functionality hinders us from understanding these biases completely which also further prevents generalization across different GCMs and locations, especially for precipitation. In this study, we propose a differentiable bias adjustment framework called δ CLIMBA (or dCLIMBA), that learns a spatiotemporally adaptive parametric bias adjustment procedure between historical CMIP6 model outputs and reference reanalysis datasets (Livneh). Results demonstrate that the proposed method accurately corrects both the magnitude and distribution of extreme storm events, with particularly strong performance in capturing extremes. The quantile distribution of precipitation is well reproduced across diverse U.S. cities, and spatial patterns perform comparably to the widely used LOCA2 statistical downscaling technique. In addition, the framework showed future trend preservation unlike pure quantile based methods and LOCA2; and results from bias correction over unseen regions showed that the marginal biases were attenuated. This work presents a modular, computationally efficient and extensible bias correction approach that is physically informed, scalable, and compatible with both historical and future applications. Its flexibility makes it suitable for integration into Earth system post-processing pipelines and impact workflows.

Keywords

Precipitation, bias correction, machine learning, circulation models, differentiable models

Highlights

1. Introduces δ CLIMBA, a differentiable framework that learns spatially and temporally adaptive monotonic transformations to bias-correct CMIP6 daily precipitation using reanalysis as reference
2. Across six CMIP6 models over CONUS, δ CLIMBA reduces marginal and extreme-precipitation biases and largely preserves multiscale spatial structure.

3. δCLIMBA partially preserves future precipitation trends and shows some spatial generalization to unseen regions.

1. Introduction

Global Circulation Models (GCMs) are essential tools for projecting future atmospheric regime change, but their outputs are subject to systematic biases that limit their direct use in regional impact assessments. These models simulate interactions between the atmosphere, hydrosphere, cryosphere, and biosphere, and are used by policymakers and scientists to develop mitigation and adaptation strategies (Intergovernmental Panel On Climate Change, 2014). Our research focuses on simulations from the Coupled Model Intercomparison Project (CMIP), which produces centennial climate projections from multiple GCMs (Eyring et al., 2016a). Fundamental insights from these simulations guide policymakers in the fields of water, energy, and biodiversity, but their applicability for local-scale impact studies is hindered by their coarse spatial resolution and intrinsic biases (Palmer & Stevens, 2019). These systematic biases which critically limit the direct use of GCMs in regional impact assessments, stem from multiple factors, including structural errors and simplifications, inaccurate parameter values, and uncertainties in forcings and boundary conditions. Approximations of sub-grid-scale processes such as cloud formation, convection, and land-atmosphere interactions create errors that may be negligible at the GCM scale (Hourdin et al., 2017), but result in systematic biases when disaggregated or interpolated to finer scales; these biases can be particularly troublesome in regions with complex topography or heterogeneous land surface properties where coarse-scale GCMs struggle to capture local variability (Giorgi & Mearns, 2002).

To enhance the applicability of GCMs on the finer scales, bias correction techniques (also referred to as bias adjustment) have often been used to adjust GCM outputs and align their properties with chosen observational datasets. Bias adjustment is carried out traditionally by methods like quantile mapping, linear scaling, and regression-based transfer functions (Piani et al., 2010). Though these traditional methods are very popular, their utility is impaired by their dependence on linear assumptions and inability to capture complex, non-linear dependencies between atmospheric variables (Ehret et al., 2012). A major limitation of these methods is that they usually depend on the assumption of a stationary relationship between model outputs and observations. As atmospheric dynamics get altered over time, the calibrations learned on historical data become inaccurate under future conditions, leading to errors in extreme event

projections (Deser et al., 2012). Traditional methods also are applied on a point-by-point basis, with no regard for spatial coherence, but maintaining realistic spatial patterns is also important, e.g., for understanding storm clustering (Hess et al., 2023; Lovejoy et al., 1987). In addition, unless special measures are taken, adjusting bias based on stationary relationships can distort the generated by the model (Buser et al., 2009; Ehret et al., 2012).

Machine learning based bias correction has recently progressed beyond traditional quantile mapping toward architectures explicitly tailored to correcting errors (Hess et al., 2023; Pan et al., 2021; F. Wang et al., 2023). For example, Hess et al., (2023) use an adversarial domain adaptation framework to learn a mapping between historical GCM simulations and observations that corrects biases while preserving spatiotemporal coherence in daily precipitation. Pan et al., (2021) demonstrate that generative adversarial networks can improve daily precipitation fields from CMIP6-class Earth system models, reducing systematic errors in means, extremes, and spatial patterns compared to standard statistical corrections. Wang et al., (2023) develop a customized convolutional neural network that incorporates physically relevant covariates, multitask learning, and weighted loss functions, showing enhanced skill relative to conventional approaches in downscaling and bias-correcting hourly precipitation, particularly for extreme events. Together, these ML-based frameworks illustrate the potential of flexible, data-driven bias correction of GCM outputs.

Despite these successes, purely data-driven ML approaches face challenges like generalization & interpretability. Like their statistical counterparts, ML approaches are trained on historical datasets, and hence are prone to overfitting and may fail to generalize across multiple GCMs. Data-driven approaches to bias correction typically produce outputs in opaque ways--- it is unclear what exact transformations they applied. They focus only on optimizing their loss functions; this can result in the disruption of overall physical consistency due to the lack of physical or (in case of precipitation) hydrological constraints (Harder et al., 2022; D. Maraun et al., 2010). Another major issue is the lack of interpretability in ML models that infers bias-corrected variables directly and function as "black boxes", making it difficult to ensure that their outputs align with established physical principles (Harder et al., 2022). ML models also require large amounts of training data, which can be scarce or inconsistent in certain regions, reducing their robustness for global applications.

To obtain an interpretable bias corrector differentiable modeling frameworks, which integrate process-based models with data-driven models. Differentiable models "refer to joint physics--NN

modelling approaches that use any method for rapidly and accurately producing gradients to achieve the large-scale optimization of the combined system” (Shen et al., 2023). These frameworks allow for automatic differentiation of parameters, enabling seamless optimization while maintaining adherence to physical principles such as conservation of energy and mass (Tsai et al., 2021). Differentiable programming has already demonstrated success in hydrological modeling and ecological simulations, offering a pathway to more interpretable and generalizable models (Aboelyazeed et al., 2023; Bindas et al., 2024; Feng et al., 2022; P. Li et al., 2024; Rahmani et al., 2023). Such frameworks have already shown potential in understanding and mitigating some biases in reanalysis datasets through parametric fusion informed by hydrology (Sawadekar et al., 2025).

Here, we develop a differentiable climate model bias adjustment (δ CLIMBA) model for daily precipitation simulated by GCMs. This method applies a parameterized transformation optimized over matching quantiles. This framework provides considerable flexibility due to its GCM- and ML-agnostic approach, and its differentiability creates the potential to study the model biases it corrects. The proposed framework improves bias adjustment of GCM outputs for variables including precipitation, which is one of the most difficult variables to bias correct or downscale due to its intermittent nature and highly skewed, non-Gaussian distribution (Hess & Boers, 2021). By leveraging large-scale reanalysis datasets, this framework learns spatial and temporal patterns of bias while incorporating the requisite constraints on the outputs. Traditional methods often struggle to maintain statistical accuracy while preserving physical coherence, particularly for extreme events and hydrologically relevant processes. Using differentiable programming, this research seeks to improve the reliability and applicability of climate simulations for water resource management and ecosystem modeling. We will also leverage the differentiable framework to bias correct precipitation in unseen regions (those without extensive ground truth data) and learn about its capability to generalize spatially since we explicitly integrate topographical attributes into our model.

To achieve this, the study focuses on the following research questions:

- ***Can the framework generalize across space and across GCMs while preserving trends ?***

- ***How well does the framework attenuate marginal biases in intensity, extremes, and threshold exceedances?***
- ***Does the framework distort spatial patterns in precipitation?***

2. Methods and Data

We used two jointly connected temporal and spatial encoders that predict coefficients for a monotonic softplus transformation of precipitation from GCM outputs, with the GCM itself and a small set of attributes serving as model inputs (Figure 1). This transformation is ‘learned’ against a quantile-based loss function (along with few more complimentary loss functions). We evaluate the overall utility of the bias-adjusted GCM output using a number of ETCCDI precipitation indices.

2.1 Differentiable Bias Adjustment Model (δ CLIMBA)

The bias adjustment here uses a differentiable model framework inspired by (Feng et al., 2022; P. Li et al., 2025)), wherein a neural network is connected to a process-based model to improve parameterization. The philosophy behind this methodology is to parameterize the transformation of GCM precipitation by optimizing the match between quantiles, with the aim of learning interpretable and generalizable mappings that can be ported to untrained locations.

The δ CLIMBA model comprises two neural networks: NN_1 and NN_2 . NN_1 is a temporal encoder which is responsible for learning biases based on temporal patterns. We evaluated several candidates for NN_1 including a simple Multi-Layer Perceptron (MLP) (P. Li et al., 2020; Rumelhart et al., 1986), a Long Short-Term memory model (LSTM) (Feng et al., 2020; Hochreiter & Schmidhuber, 1997), and a one-dimensional Convolutional Neural Network (CNN-1d) (Feng et al., 2021; LeCun et al., 1989; P. Li et al., 2024) that would generate parameters to facilitate the GCM’s transformation. NN_2 is an attention-based (Vaswani et al., 2017) spatial encoder that learns spatial relationships between neighboring inputs. The spatial self-attention is performed independently at each time step over the nodes within a patch, where queries, keys, and values are derived from node features and augmented with a learnable, head-specific offset that encodes pairwise geodesic relationships (i.e., relative displacement, distance, and bearing). This formulation allows the model to adaptively weight neighboring nodes based on physically meaningful spatial geometry rather than relying on fixed or isotropic

spatial kernels. For each grid cell, we choose the 16 nearest neighbors whose time series are positively correlated with that of the target grid cell. Our final model configuration uses a CNN-1d with 2 hidden layers of size 64 for NN_1 , and a Transformer with a self-attention mechanism employing 2 attention heads and 64 model (hidden) dimensions for NN_2 . We trained the model using the Adam optimization (Kingma & Ba, 2017) algorithm with a learning rate at $1e-4$. This configuration was chosen based on overall performance across different precipitation indices.

The full process can be mathematically described as:

$$NN_{BA}(X, A, X_{t-1}, X_{t-2}, X_{t-3}, I_t) = [\alpha, w, s, b, c] \equiv \theta \quad (1)$$

$$X_{BA} = \alpha x + \sum_{z=1}^Z w_z \text{softplus}(s_z(x - b_z)) + c \quad (2)$$

Here X is GCM precipitation of the shape (batch size, neighbors, time,). I_t is wet day indicator where $I_t = 1$ if daily precipitation (X) ≥ 1 and $I_t = 0$ otherwise. NN_{BA} is the jointly connected network of NN_1 and NN_2 . A is the list of static attributes that could logically influence bias in precipitation such as elevation, slope, aspect, and land cover.

The output of NN_{BA} is a set (θ) of temporally- and spatially-varying parameters (α, w_z, s_z, b_z, c) for the ‘softplus monotone basis’ mapping, which enforces monotonicity through softplus-based basis bumps (Zhou, 2016). Z is the number of basis bumps (a hyperparameter tuned to 8). X_{BA} is the resulting bias-corrected GCM precipitation.

We used the following composite loss function in training:

$$L = p_1 * Q + p_2 * R + p_3 * S \quad (3)$$

Here, L (the total loss) combines three components: quantile-based loss (Q), rainy-day loss (R), and spatial correlation loss (S). These components were weighted with $p_1 = 0.99$, $p_2 = 0.01$ and $p_3 = 1$. This formulation is designed to ensure overall distributional similarity while also paying attention to spatial structures and rainy-day occurrence during model training. A description of individual loss components follows:

$$Q = \frac{1}{K} \sum_{k=1}^K g(q_k) \cdot |Q_X(q_k) - Q_Y(q_k)| \quad (4)$$

Here $Q_X(q_k)$ is the value of the empirical quantile function (inverse CDF) of data X at quantile level q_k ; $Q_Y(q_k)$ represents the same but for reference data Y . K is the number of quantile levels used (1000), and q_k are the uniformly-spaced quantile levels. The weights $g(q_k)$ allow emphasis on specific quantiles; we used the kernel function

$$g(q_k) = \exp(-|q_k - q^*|) \quad (5)$$

where q^* is quantile we want to emphasize. This is particularly useful for precipitation, where it is important to correct bias in the extremes as well as the bulk of the distribution. If no emphasis is specified, then $g(q_k) = 1$ (uniform). We treated q^* as a hyperparameter in our training, choosing a value of either 0.5 or 0.9 for each GCM based on performance.

The second component is the rainy-day loss function, which is a soft constraint formulated to preserve the frequency of wet/dry days in the data.

$$R = \frac{1}{N} \sum_{i=1}^N \left| \sum_t \sigma(X_{it} - \alpha) - \sum_t \sigma(Y_{it} - \alpha) \right| \quad (6)$$

Here, X_{it} and Y_{it} are bias-adjusted and reference data, respectively, for sample i and time t . σ is the sigmoid function which provides a differentiable approximation of the indicator function for rainy/wet days. α is the wet day threshold (1 mm). N is the number of samples or sites.

The third component is the spatial correlation loss, which is a constraint added to preserve spatial structures in the bias corrected simulation.

$$S = \frac{1}{BT} \sum_{b=1}^B \sum_{t=1}^T (1 - \text{correlation}(X_{b,t}, Y_{b,t})) \quad (7)$$

$$\text{correlation}(X_{b,t}, Y_{b,t}) = \frac{\sum_{p=1}^P Y_{b,p,t} X_{b,p,t}}{\sqrt{\sum_{p=1}^P Y_{b,p,t}^2 + \epsilon} \sqrt{\sum_{p=1}^P X_{b,p,t}^2 + \epsilon}} \quad (8)$$

Here, B is the number of batches, T is the total number of time steps, and P is the number of neighbors for each of the coordinates in B . ϵ is a small constant (e.g., 10^{-8}) to prevent division by zero.

Because every GCM has a distinctive, characteristic large-scale bias pattern (Krinner & Flanner, 2018), no single bias adjustment transformation will be suitable for all GCMs. We therefore performed multiple training runs for each GCM, allowing hyperparameters like q^* and the number of training epochs to vary. We choose the best configuration for each GCM by analyzing quantile loss and ETCCDI indices in the validation set. For every candidate configuration, we first checked if the quantile loss is monotonically decreasing with epochs and then we calculated the ETCCDI indices described in section 2.4 for the validation period, then computed a composite score defined as the mean percentage bias across all indices, and selected the hyperparameter set with the lowest composite score for that GCM.

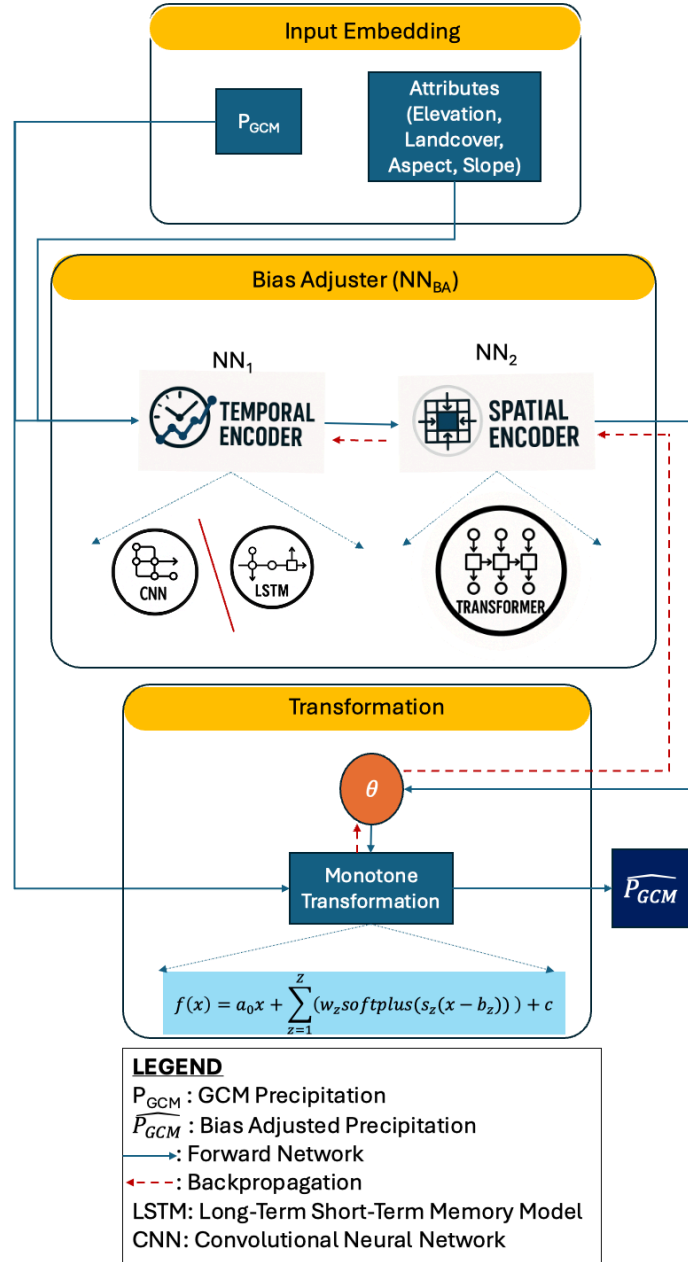


Figure 1. Schematic of the δ CLIMBA framework for differentiable precipitation bias adjustment. Raw GCM precipitation (P_{GCM}) and static spatial attributes (elevation, land cover, aspect, slope) are embedded and passed to a bias-adjustment network (NN_{BA}). The network consists of temporal and spatial encoders which jointly estimate parameters θ governing a monotonic transformation ($f(x)$). The transformation module applies a learnable, differentiable monotone mapping to produce bias-adjusted precipitation (\widehat{P}_{GCM}) based on the feedback from the composite quantile loss function.

2.2 Datasets

We employed daily precipitation data from Coupled Model Intercomparison Project Phase 6 (CMIP6) (Eyring et al., 2016b) model outputs from historical experiments and future scenario with high emissions and stronger reliance on fossil fuels i.e., Shared Socioeconomic Pathways (SSP 585). For the current scope, the following six CMIP6 models were selected: ACCESS-CM2, GFDL-ESM4, IPSL-CM6A-LR, MIROC6, MPI-ESM1-2-LR, and MRI-ESM2-0 for bias correction of their precipitation. Each of these models were used at their native resolution (1° to 2.5° ; refer Table 1) within the CONUS region at the daily timescale for historical simulation.

We considered using gridded Livneh (Livneh et al., 2013) data as reference for comprehensive evaluation of our model over the entire CONUS. For the current work, both of these datasets were upscaled (spatially) from the original resolution of $1/16^\circ$ to the resolution of the respective CMIP6 members. For direct comparison with LOCA2, we used unsplit-Livneh (Pierce et al., 2021) which was used as reference for the development of the same.

The Localized Constructed Analogs (LOCA2) dataset (Pierce et al., 2014, 2021) is considered as a very important resource for downscaled products of CMIP6 (Vano et al., 2020). It presents a downscaled product with substantially improved resolution of $1/16^\circ$ degree grid as it was calibrated using unsplit-Livneh. LOCA2 leverages spatial analog approaches to match patterns from regional to local-scale features. Due to its ubiquity in our target CONUS region and thoroughly vetted by evaluations (Ullrich, 2023), we decided to use it as a benchmark product against our differentiable approach along with other bias correction methods. To use this, we upscale LOCA2 to GCM's spatial resolution to evaluate purely for systemic biases.

Furthermore, input features like elevation, aspect, slope, and landcover were used to assist precipitation bias adjustment. Elevation, slope, and aspect were extracted from Digital Elevation Models at 0.01° resolution from NASA Shuttle Radar Topography Mission Global 1 arc second V003 dataset (SRTMGL1) (NASA JPL, 2013). Landcover data was produced from Landsat at 30m US coverage and downloaded from CEC's North American Land Change Monitoring System (NALCMS) (Pasos, 2020). All of these data features were regridded to respective GCMs from CMIP6 to match the domain.

Table 1. Description of Global Climate Models (GCMs)

| Short Name | Full Name | Institution/consortium | Native Resolution |
|---------------|--|--|-------------------|
| ACCESS-CM2 | Australian Community Climate and Earth System Model version 2 | CSIRO / Bureau of Meteorology / Australian universities (ACCESS community) (Bi et al., 2020) | ~1.25° x ~1.87° |
| GFDL-ESM4 | Geophysical Fluid Dynamics Laboratory Earth System Model 4 | NOAA Geophysical Fluid Dynamics Laboratory (NOAA-GFDL) (Krasting et al., 2018) | ~1.00° x ~1.25° |
| IPSL-CM6A-LR | Institut Pierre-Simon Laplace Climate Model version 6A, low resolution | Institut Pierre-Simon Laplace (IPSL), France (Boucher et al., 2018) | ~1.26° x ~2.50° |
| MIROC6 | Model for Interdisciplinary Research on Climate version 6 | MIROC consortium: JAMSTEC, AORI (Univ. Tokyo), NIES, R-CCS Kobe, others (Mochizuki et al., 2019) | ~1.40° x ~1.40° |
| MPI-ESM1-2-LR | Max Planck Institute Earth System Model version 1.2, low resolution | Max Planck Institute for Meteorology (MPI-M), Germany (Gutjahr et al., 2019) | ~1.87° x ~1.87° |
| MRI-ESM2-0 | Meteorological Research Institute Earth System Model version 2.0 | Meteorological Research Institute (MRI), Japan (Kawai et al., 2019) | ~1.12° x ~1.12° |

2.3 Experiment Design

We trained the model on the period 1979–2000 and validated it on the period 1965–1978. We tested bias-corrected outputs of the GCMs over the period 2001–2014. For the evaluation of future scenarios, we choose Shared Economic Pathways (SSP5-8.5) (Intergovernmental Panel On Climate Change (Ipc), 2023) for the period 2015–2099. We interpolated the reference data (unsplit-Livneh) using nearest-neighbor interpolation to the resolution of each GCM before using it for modeling.

We evaluated the model by comparing it to a set of five bias-correction methodologies detailed in Table 2.

Table 2. Summary of the Bias Adjustment methods used for evaluation. All methods except LOCA2 were implemented using the ‘ibicus’ framework proposed in (Spuler et al., 2024).

| Method | Description |
|------------------------------|--|
| Quantile Mapping (QM) | Statistical bias correction that adjusts the modeled distribution so its quantiles match those of observations (Cannon et al., 2015; Douglas Maraun, 2016). |
| ISIMIP (ISIMIP3BASD) | Trend-preserving bias adjustment and statistical downscaling framework developed for the Inter-Sectoral Impact Model Intercomparison Project; uses parametric/nonparametric quantile mapping tailored to each variable, with explicit preservation of trends across quantiles and options for multivariate/space-time structure (Lange, 2019). |
| ECDFM | Nonparametric quantile mapping where empirical CDFs are used and the correction is applied as an additive (or multiplicative) “distance” between modeled and observed quantiles (H. Li et al., 2010; L. Wang & Chen, 2014). |
| Quantile Delta Mapping (QDM) | Bias-correction method that corrects biases at each quantile while explicitly preserving the modeled climate-change signal at that quantile (Cannon et al., 2015; L. Wang & Chen, 2014). |
| LOCA2 (upscaled) | Updated hybrid statistical downscaling method that extends LOCA: uses an analog-based constructed-analog framework with observational training data, two-step coarse-to-fine downscaling, and explicit seasonal, intensity-dependent bias correction (Pierce et al., 2021). |

We performed our experiments on the Perlmutter system at NERSC. For training on six GCM members across CONUS for 100 epochs on different hyperparameter combinations distributed over 4 A100 GPUs parallel, it took 7 hours of time. While it took 2 minutes for the inference to produce bias corrected simulation across CONUS in testing and future period.

2.4 Evaluation Design and Metrics

For a comprehensive evaluation of our model, we focus on investigating the characteristics of bias corrected simulations through Expert Team on Climate Change Detection and Indices (ETCCDI) for marginal biases, fractal dimension for spatial patterns/clustering, and trend bias percentage.

To evaluate the temporal structure and marginal biases of the corrected data, we calculate the ETCCI indexes listed in Table 3. To place the different GCMs and bias adjustment methods on

an equal footing during the evaluation, we first interpolate all of the bias-adjusted simulations to the resolution of the coarsest GCM (IPSL-CM6A-LR, 1.25°x2.5°).

Table 3. Summary of ETCCDI Indices for precipitation evaluation

| ETCCDI Indices | Definition |
|-------------------------------------|---|
| R10mm | Annual count of days when precipitation $\geq 10\text{mm}$ |
| R20mm | Annual count of days when precipitation $\geq 20\text{mm}$ |
| Rx1day | Monthly maximum 1-day precipitation amount |
| Rx5day | Monthly maximum 5-day precipitation amount |
| Simple Daily Intensity Index (SDII) | Monthly average precipitation amount on wet days (precipitation $\geq 1\text{mm}$) |
| Consecutive Dry Days (CDD) | Annual maximum number of consecutive days with precipitation $< 1\text{mm}$ |
| Consecutive Wet Days (CWD) | Annual maximum number of consecutive days with precipitation $\geq 1\text{mm}$ |
| R95pTOT | Annual total precipitation from days exceeding the 95th-percentile of daily precipitation during a reference period |
| R99pTOT | Annual total precipitation from days exceeding the 99th-percentile of daily precipitation during a reference period |

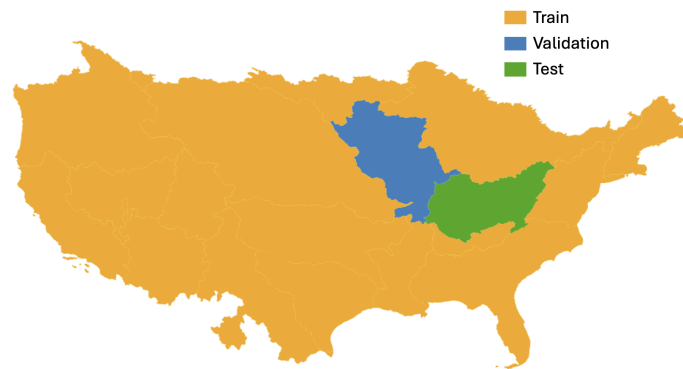


Figure 2. Spatial configuration of training, validation, and test domains used to evaluate δCLIMBA in data-scarce settings. Validation and test regions are withheld entirely from model training.

To evaluate spatial structure, we use the scale-dependent fractal dimension (FD) computed via the box-counting method (Husain et al., 2021; Lovejoy et al., 1987; Meisel et al., 1992) applied to thresholded binary precipitation fields at each quantile level. This method has been already

used in the past to study how precipitation patterns change across scales (Hess et al., 2023; Lovejoy et al., 1987). For a given quantile threshold t , the precipitation field Z is converted to a binary mask B_t :

$$B_t = \{1 \text{ if } Z \geq t \text{ else } 0\} \quad (9)$$

To measure how this thresholded pattern occupies space across scales, the mask is then partitioned using square boxes of side length ϵ . For each ϵ , we count the number of partially filled boxes, $N(\epsilon)$, i.e., boxes that are neither empty nor completely full. If fractal scaling is assumed as,

$$N_\epsilon \propto \epsilon^{-FD} \quad (10)$$

Then

$$FD = \frac{\log(N_\epsilon)}{\log(1/\epsilon)} \quad (11)$$

Hence, FD is determined from the negative slope of $\log(N_\epsilon)$ and $\log(\epsilon)$.

For evaluating changes in climate signal trend, we use the framework from the 'ibicus' package ((Spuler et al., 2024). For a particular GCM and bias-correction method, we first compute the raw trend for a statistic S (e.g., mean or 95th quantile) between the future (2015–2099) and historical (1980–2014) periods:

$$T_{raw} = S_{raw, future} - S_{raw, historical} \quad (12)$$

Then, we calculate the trend after carrying out bias adjustment:

$$T_{debiased} = S_{debiased, future} - S_{debiased, historical} \quad (13)$$

Finally, the trend bias (TB) is calculated as the percentage change between T_{raw} and $T_{debiased}$:

$$TB = 100 \cdot \frac{T_{debiased} - T_{raw}}{T_{raw}} \quad (14)$$

One of the advantages of this differentiable framework is its ability to generalize not only in time but in space, provided we ingest data that helps it to learn spatial context (e.g., elevation, slope, and landcover). Our final evaluation was a spatial test where we trained, validated, and tested the model on different regions as shown in Figure 2. We trained and evaluated the model on the period 1990–2014, holding out the Upper Mississippi region (blue) for validation to select

hyperparameters, and used this learned configuration to test in the adjacent Ohio region (green).

3. Results

δ CLIMBA was evaluated using a series of experiments to test its generalizability across different GCMs at different locations, including its ability to adjust biases through precipitation indices, conserve spatial structures and long term trends.

3.1 Quantile Comparison

Quantile comparisons across five climatically diverse U.S. cities demonstrate that δ CLIMBA systematically aligns the daily precipitation distributions of all six CMIP6 models with the Livneh reference across the full distributional range, including the upper tail, without inducing the nonphysical amplification of extremes that is characteristic of several conventional adjustment methods. Figure 3 presents empirical quantile curves for raw and bias-adjusted CMIP6 output evaluated at five cities spanning arid, mountainous, maritime, humid subtropical, and temperate climatic regimes (Phoenix, Yosemite, Seattle, Orlando, and Philadelphia, respectively).

While the raw models exhibit large spread and biases compared to observations, δ CLIMBA consistently aligns model quantiles with the reference across the full distribution while preserving relative inter-model differences and avoiding artificial tail inflation (Figure 3). The raw models' large inter-model spread and systematic biases are strongly regime-dependent: most models generally match reanalysis in Philadelphia, but display dry-region overestimation in Phoenix, exaggerated tails in mountainous Yosemite, and inconsistent heavy-rain behavior in humid Seattle and Orlando. Conventional bias-correction methods reduce mean bias but frequently distort tail behavior: Quantile Mapping, ISIMIP, and ECDFM often over-amplify upper quantiles, while Quantile Delta Mapping produces unstable and occasionally explosive tails (most evident in Phoenix and Orlando). LOCA2 improves inter-model consistency but still shows city-dependent residual biases in extremes. δ CLIMBA performs well across multiple regimes and GCMs, indicating that the differentiable, spatially conditioned formulation corrects distributional bias without inducing nonphysical extreme amplification, a failure mode clearly visible in several traditional methods.

Quantile Comparison across Cities x Methods

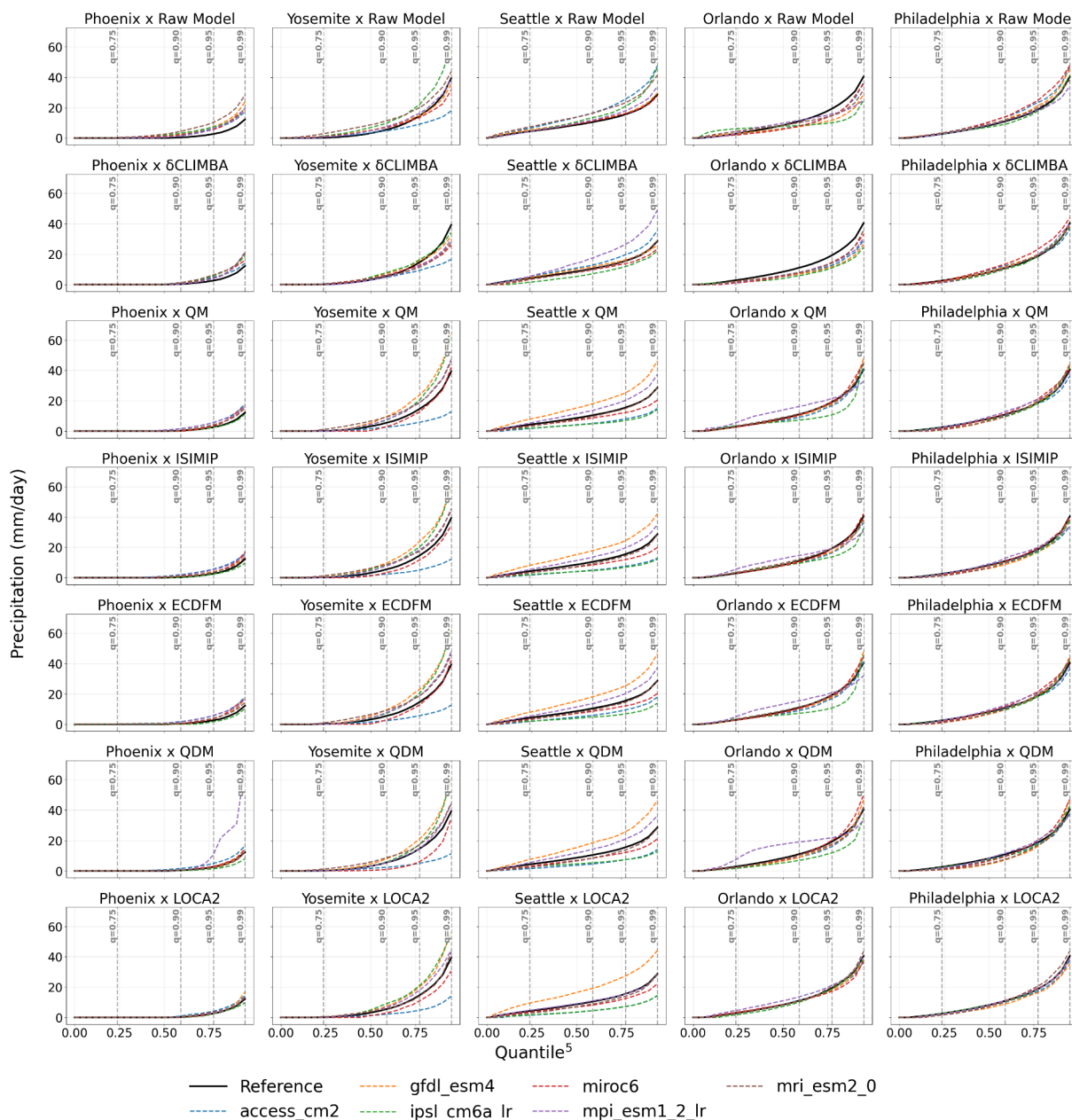


Figure 3. Quantile comparison of daily precipitation across selected cities and bias-adjustment methods during the test period (2001–2014). For each city–method combination, empirical quantile curves of the six CMIP6 GCMs are shown alongside the Livneh reference distribution. The x-axis displays quantiles to the 5th power to expand the upper tail and emphasize extreme precipitation behavior. The y-axis represents precipitation (mm day⁻¹). Columns correspond to different cities and rows to bias-adjustment methods.

3.2 Precipitation Indices

Across nearly all indices, including intensity (Rx1day, Rx5day), threshold exceedance (R10mm, R20mm), persistence (CDD, CWD), and extreme totals (R95pTOT, R99pTOT); δ CLIMBA exhibits a narrower spread and a median bias closer to zero compared to traditional statistical methods, as shown in Figure 4. In contrast, raw model output and several conventional corrections show large positive biases for extreme and heavy-precipitation indices, as well as substantial dispersion, highlighting their limited ability to jointly control mean bias and spatial consistency.

While Figure 4 summarizes the distribution of grid-wise biases, it does not reveal whether residual errors exhibit coherent spatial structure. Figure 5 therefore examines the spatial distribution of mean percentage bias across CONUS for selected ETCCDI indices. This analysis allows assessment of whether δ CLIMBA merely reduces aggregate bias or also mitigates geographically systematic error patterns.

Across all metrics except CDD, the raw GCM output exhibits widespread positive bias over CONUS. While conventional bias adjustment methods such as Quantile Mapping (QM) effectively reduce this bias, their performance varies substantially across regions. For instance, QM retains positive residual bias in the southeastern United States relative to both LOCA2 and δ CLIMBA for multiple extreme metrics including R99pTOT, SDII, Rx5day, and CWD.

For extreme precipitation totals (R99pTOT), QM exhibits pronounced positive bias across the entire region. In contrast, δ CLIMBA mitigates these extremes without introducing systematic negative compensation elsewhere, indicating that its learned monotonic transformation adapts spatially. This behavior aligns with the spatial conditioning embedded in the neural architecture which enables to gain spatial context while attenuating bias. In addition to that, the weighted quantile loss function (giving more penalty to higher quantiles) gives direct feedback to model to debias precipitation at higher end of the distribution. While LOCA2 achieves comparable performance to δ CLIMBA, it retains moderately higher residual bias across CONUS.

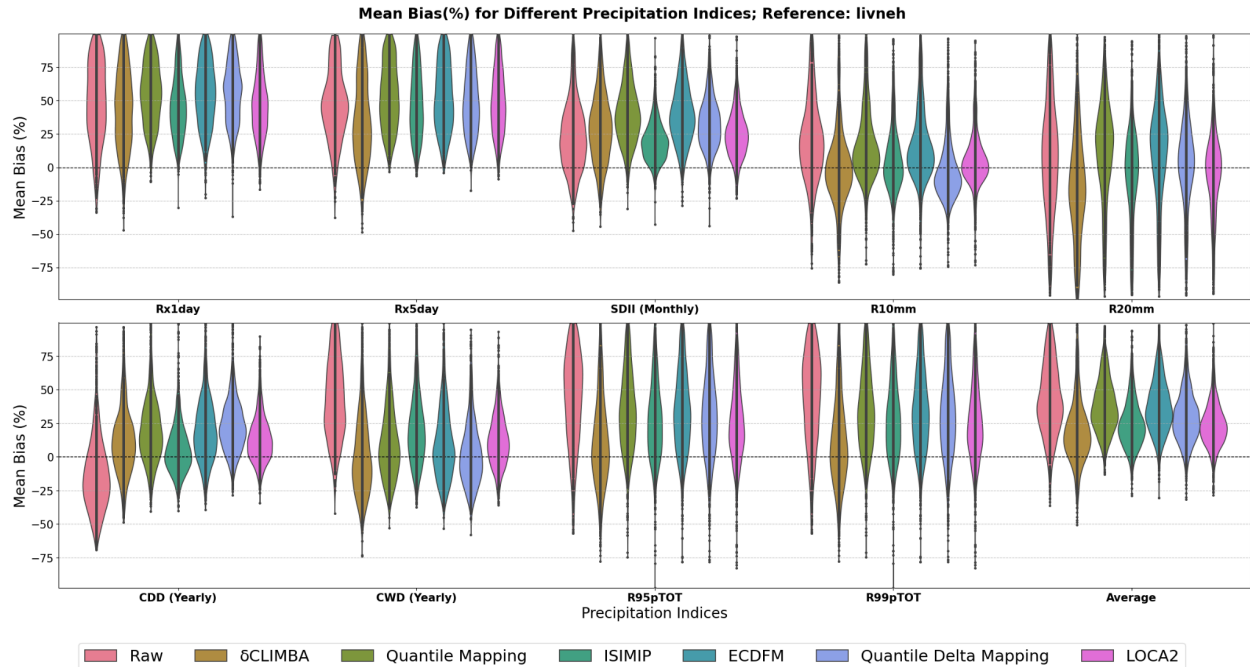


Figure 4. Spatial Distribution of mean percentage bias for ETCCDI precipitation indices over CONUS during the test period (2001–2014), evaluated against the Livneh reference dataset. Results are shown for the ensemble of six CMIP6 GCMs. Each violin represents the distribution of grid-point mean percentage bias across CONUS for a given index and method. The “Average” column reports the arithmetic mean of mean percentage bias across all ETCCDI indices for each method. Narrower distributions and medians closer to zero indicate improved bias stability and reduced spatial heterogeneity.

Intensity and frequency-based indices (SDII and R20) remain challenging for all approaches. For SDII, bias adjustment techniques counterintuitively increase bias relative to raw CMIP6 output rather than reducing it. This degradation is most pronounced in the central United States, where QM introduces the largest bias amplification, while LOCA2 and δ CLIMBA exhibit comparable residual bias. The threshold-based index R20 presents a distinct challenge: unlike other metrics, it exhibits systematic underestimation, particularly across the western mountainous region. Nevertheless, δ CLIMBA and LOCA2 successfully reduce positive bias at many R20 locations, suggesting that the monotonic transformation constraint preferentially suppresses high-frequency precipitation events.

Spatial Bias Across Precipitation Indices

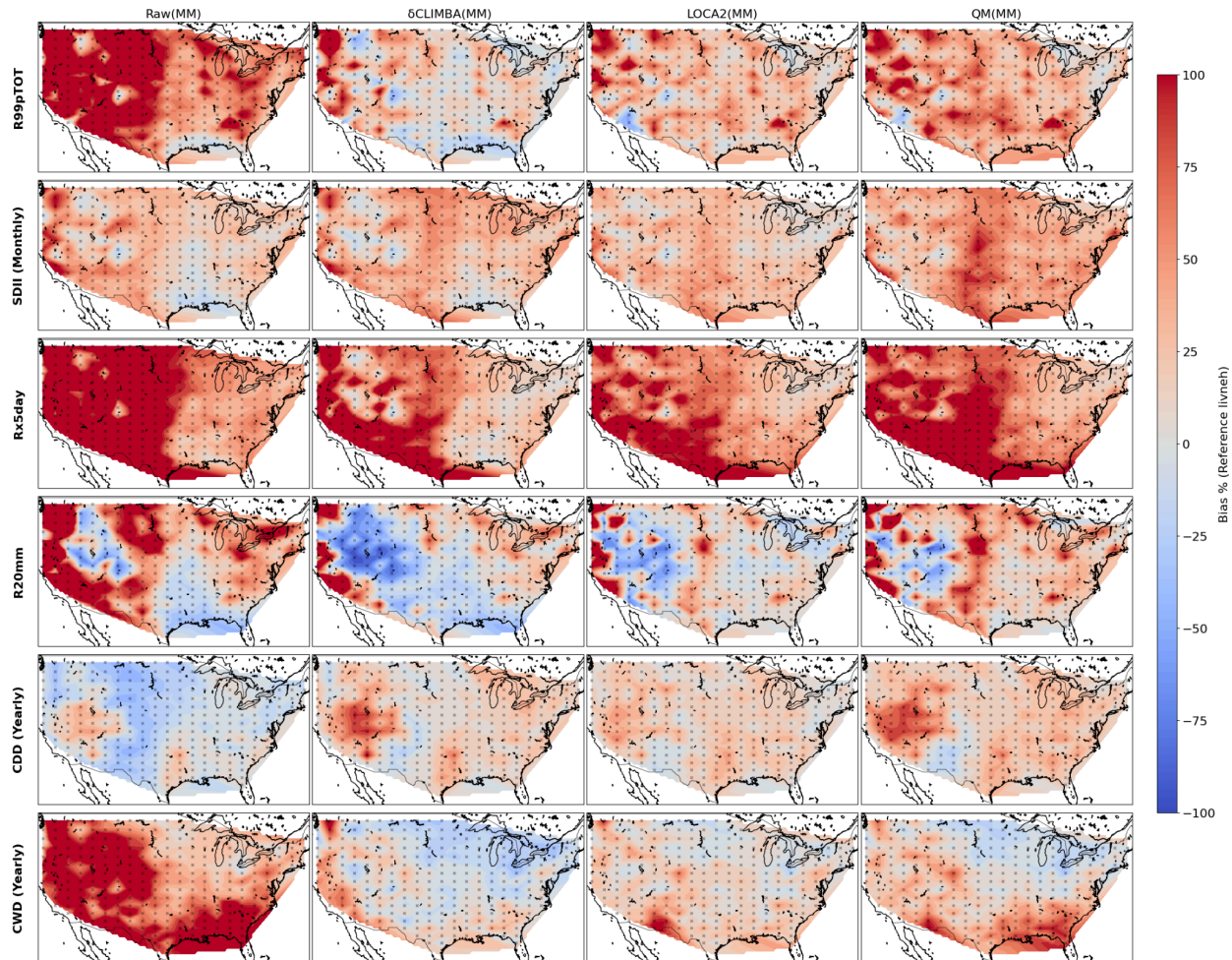


Figure 5. Spatial distribution of mean percentage bias (%) for selected ETCCDI precipitation indices over CONUS during the test period (2001–2014), evaluated against the Livneh reference dataset. Results are shown for the ensemble mean (model mean, MM) of six CMIP6 GCMs. Rows correspond to precipitation indices, and columns correspond to bias-adjustment methods. Positive values indicate overestimation relative to Livneh, and negative values indicate underestimation. This figure highlights the spatial structure of residual bias, complementing the distributional summaries shown in Figure 3.

All approaches achieve substantial bias reduction for both temporal sequencing metrics (CDD and CWD) across CONUS. For CWD, positive bias is effectively attenuated throughout most of the domain, with persistent residual bias limited to a few west coast locations. Both δ CLIMBA and LOCA2 outperform QM in the high-rainfall southeastern region. For CDD, negative bias is similarly reduced across most locations, though a cluster of grid points in the western interior retains positive residual bias across all methods.

Collectively, these spatial diagnostics reveal heterogeneous performance of δ CLIMBA across different precipitation characteristics. The method achieves consistent improvements in extreme totals (R99pTOT) and temporal sequencing metrics (CDD, CWD), while matching or exceeding LOCA2's performance and substantially outperforming conventional QM. Since GCMs usually tend to carry systematic wet (positive) biases (Srivastava et al., 2020), the transformation in δ CLIMBA seems particularly amenable in mitigating positive bias; especially in regions like the southeastern US where precipitation distribution is highly skewed and frequency and intensity is driven by mesoscale convective systems (Rahman et al., 2023). However, intensity-based indices (SDII, R20) remain challenging for all bias correction approaches, highlighting the need for methods that can explicitly account for changes in precipitation event structure.

3.3 Spatial Patterns

δ CLIMBA substantially preserves the multiscale spatial structure of precipitation fields, achieving a mean absolute error (MAE) of 0.021 relative to the Livneh reference FD curve, a marked improvement over raw CMIP6 output (MAE=0.040) and approaching the performance of LOCA2 (MAE=0.017) as shown in Figure 6. This result is notable because conventional univariate bias adjustment methods, operating independently at each grid point, lack any mechanism for learning spatial relationships and therefore tend to attenuate marginal bias at the cost of degrading spatial organization (Allard et al., 2025; Douglas Maraun et al., 2017). The fact that δ CLIMBA achieves competitive spatial fidelity without an explicit analog procedure suggests that geodesic-aware spatial attention in the spatial encoder is capturing meaningful inter-node structure during training.

While LOCA2 achieves the lowest overall MAE (0.017), δ CLIMBA competitively tracks the reference fractal-dimension curve across nearly the entire quantile range, with substantially reduced error relative to the raw model (MAE = 0.021 vs. 0.030). It exhibits good performance across the distribution, except for a deviation in the upper tail that is likely due to numerical instability, indicating that the differentiable framework corrects biases while retaining physically realistic multiscale spatial structure. LOCA2's superior MAE is consistent with its design: the spatial analog method explicitly maps regional precipitation patterns to local scales and thus inherently reproduces aspects of spatial intermittency as a direct consequence of its construction, rather than as an emergent property of learned representations.

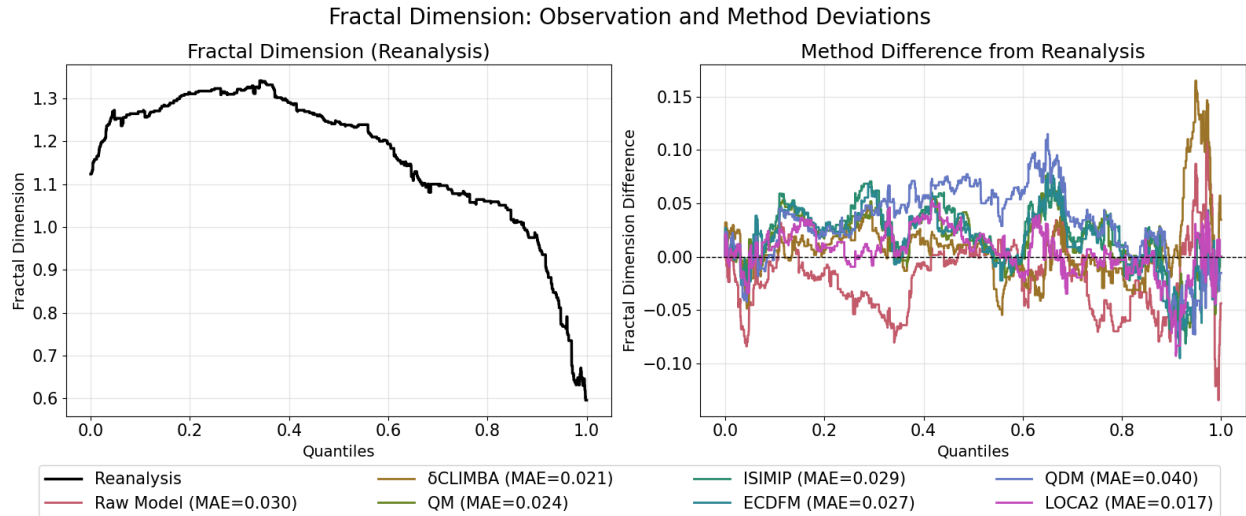


Figure 6. Fractal dimension of precipitation fields as a function of quantile over CONUS during the test period (2001–2014). The black curve represents the Livneh reference dataset, while colored curves correspond to ensemble model mean (MM) fields after bias adjustment (δ CLIMBA, LOCA2, Quantile Delta Mapping) and raw GCM output. Mean absolute error (MAE) values reported in the legend quantify deviation from the reference fractal dimension curve across quantiles.

3.4 Trend Analysis

δ CLIMBA partially preserves trend in projected precipitation for GFDL-ESM4 under SSP585 without any explicit trend-preservation mechanism embedded in the framework, outperforming QDM and LOCA2 across all evaluated metrics while trailing ECDFM and ISIMIP for mean precipitation and the 95th percentile. However, this behavior does not generalize consistently across GCMs, indicating that trend preservation is an emergent rather than a structural property of the current framework and remains an open limitation.

Figure 7 shows the bias in projected precipitation trends between the historical (1970-2014) and future periods (2015-2099) under SSP585 for mean precipitation, 95th percentile, wet days ($> 1 \text{ mm day}^{-1}$), and very wet days ($> 10 \text{ mm day}^{-1}$) across multiple bias-adjustment methods. Quantile Delta Mapping (QDM) and LOCA2 (resolution upscaled) exhibit pronounced negative trend biases across all metrics, indicating systematic attenuation of trends after bias correction. Quantile Mapping does better than its counterparts in preserving the trend of mean and 95th percentile, lags behind for wet days, and performs comparably for trend in very wet days ($>10\text{mm}$).

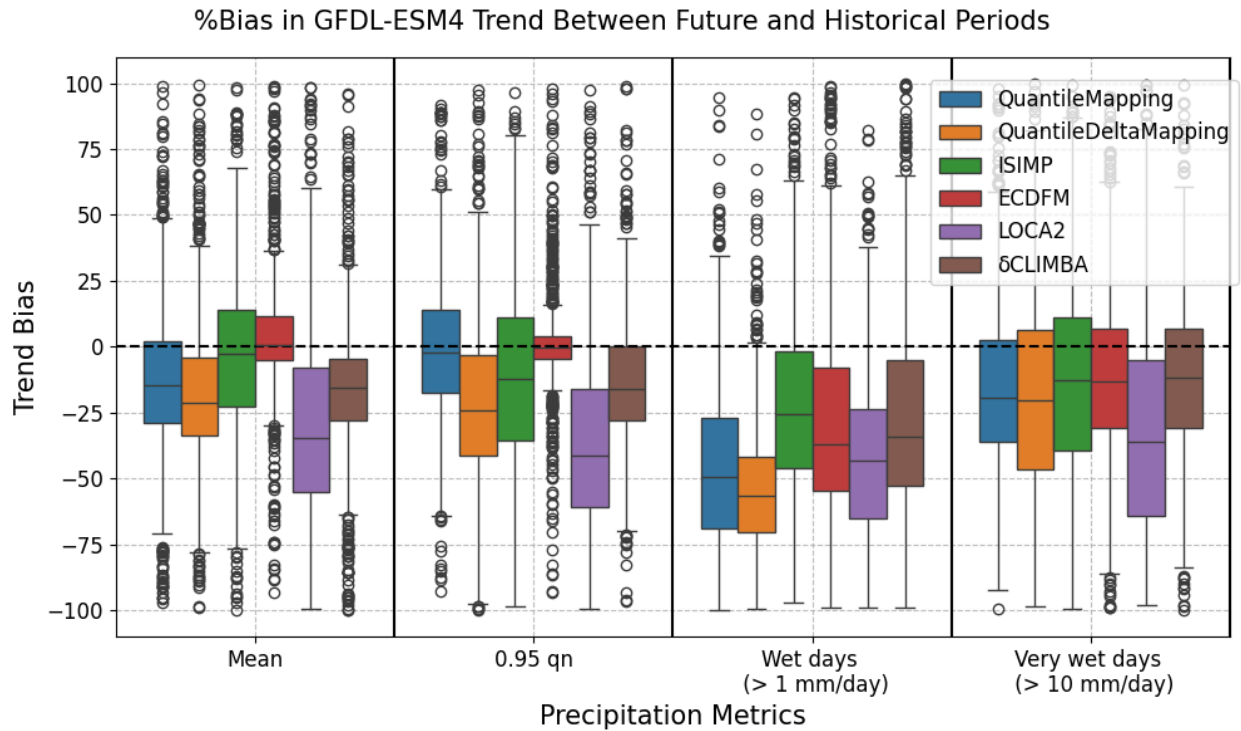


Figure 7. Percentage bias in projected climate trends of GFDL-ESM4 between future and historical periods under SSP5-8.5, evaluated across precipitation metrics over CONUS. Values closer to zero indicate improved preservation of trends following bias adjustment.

ECDFM, which is recognized for its trend preservation (H. Li et al., 2010), does a particularly good job with trend bias in the mean and 95th percentile, although its performance is more typical when evaluated for trend in number of wet days and very wet days. ISIMIP, another bias-correction method designed for trend-preservation, displays similar performance to ECDFM, though with a higher inter-quartile range, implying a larger number of locations with distorted trends.

δCLIMBA has no built-in trend-preservation mechanisms, but shows acceptable performance nonetheless. For mean and 95th percentile, it performs similarly to the two quantile-mapping methods, lagging behind ISIMIP and ECDFM but doing better than LOCA2, while for wet and very wet days, its performance is competitive with ISIMIP and ECDFM. It exhibited similar performance on some other GCMs, like ACCESS-CM2, but not all, indicating that the differentiable framework is unable to generalize the trend-preservation behaviour across GCMs.

3.5 Bias Correction in Data Scarce Regions

As shown in Figure 8, δ CLIMBA demonstrates meaningful spatial generalization to an entirely withheld region, reducing positive bias in extreme precipitation indices including R99pTOT and Rx5day without any local calibration except for validation, although indices sensitive to daily wet-day intensity (SDII, R20mm) exhibit residual overestimation, indicating a limit on the spatial transferability of the current framework.

Improvements are most pronounced for intensity-based and percentile-based indices, including Rx1day, Rx5day, and high-percentile precipitation (R95pTOT and R99pTOT) totals, indicating that the learned monotonic transformation effectively corrects systematic distributional distortions in unseen regions. Some indices, such as SDII, CDD and CWD, retain wider bias distributions, suggesting that duration-based metrics remain more challenging to correct under spatial holdout. However the longer interquartile range in the violin plots for all indices exhibit that many of the coordinates in the test region tend to end up with biases even bigger than raw simulation, like in SDII, R10, and CDD.

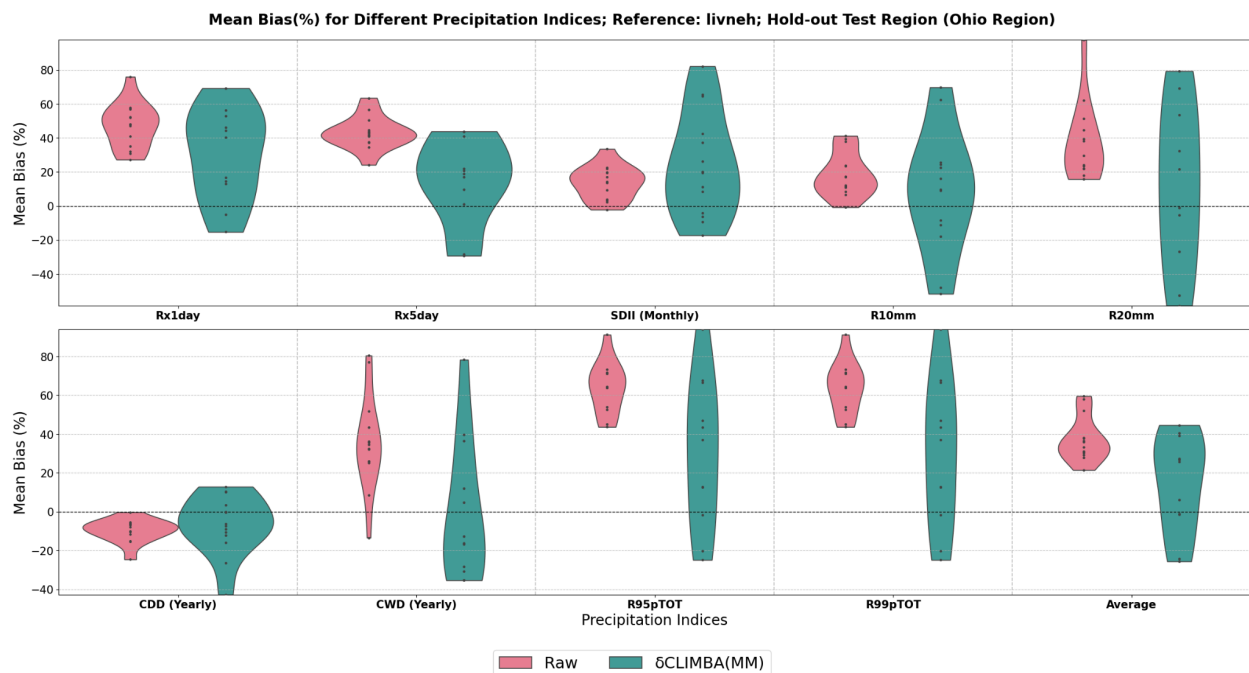


Figure 8. Spatial Distribution of mean percentage bias for ETCCDI precipitation indices over testing region (Ohio region), evaluated against the Livneh reference dataset. Results are shown for the ensemble mean (model mean, MM) of six CMIP6 GCMs. Each violin represents the distribution of grid-point mean percentage bias across CONUS for a given index and method. The “Average” column reports the arithmetic mean of mean percentage bias across all ETCCDI indices. Narrower distributions and medians closer to zero indicate improved bias stability and reduced spatial heterogeneity.

This experiment constitutes a particularly stringent test of the framework, as conventional bias-correction methods, whether distribution-based, moment-scaling, or spatial analog are explicitly calibrated against local observations and lack a principled mechanism for spatial generalization; their performance degrades outside the calibration domain by construction, making a like-for-like spatial comparison uninformative. In addition, LOCA2 is a bespoke product (Pierce et al., 2014, 2021), so there is no way to test its ability to generalize spatially.

Overall, these results demonstrate that δ CLIMBA is able to spatially generalize to some extent. Since the coordinates are moving towards zero bias, the differentiable framework has the potential to maintain stable bias-adjustment behavior when transferred to an unseen but adjacent region, reducing distributional biases without access to local calibration data.

4. Conclusions

Bias correction or bias adjustment is a field that cannot be addressed or optimized by a single metric. Every GCM output carries different kinds of biases, and therefore an exhaustive evaluation of not only marginal biases but their temporal, spatial and scale-dependent inherent characteristics is important. Section 3 therefore dives into evaluation beginning from CDF curves to trend preservation, presenting a comprehensive evaluation of the differentiable framework δ CLIMBA against traditional bias correction methods including the gold standard downscaling product of LOCA2 which we upscaled to the GCM's resolution.

We begin with analyzing power transformed CDF curves (quantiles raised to 5th power to emphasize upper quantiles) across five distinct cities of Phoenix, Yosemite, Seattle, Orlando, and Philadelphia. The differentiable framework exhibited similar behavior to the best of LOCA though lags behind in cities like Orlando, where though the GCM curves move near reanalysis, they don't overlap as well as LOCA2. On the other hand, in cities like Yosemite and Seattle, the CDF curves of GCMs collapse near reanalysis better than all the methods, even surpassing LOCA2.

In addition to that, for overall evaluation we resorted to evaluating the ensemble mean of six chosen GCMs to assess the generalizability of the methods across GCMs. δ CLIMBA excels in attenuating CONUS-wide biases in extreme totals (exhibited by R99pTOT and R95pTOT) indicating the biases in tail or the marginal behaviour are addressed by the parametric

monotonic transformation. In addition to that, the differentiable framework seems more suited to work on debiasing positive bias as is especially evident in regions like the southeastern US. However, intensity based indices like SDII remain a challenge; indicating the monotonic transformation may not be able to efficiently mitigate bias in higher quantiles even though annual precipitation is matched. This could mean that δ CLIMBA is inflating the tail of wet-day intensity distribution relative to the reference reanalysis, i.e., mapping too much probability mass into higher quantiles.

The differentiable framework δ CLIMBA uses a spatial encoder of Transformer to learn spatial structures from neighboring grid cells. Though the current framework does not help the model to learn long range spatial dependencies, this mechanism could help the model in learning spatial patterns which is essential for multiscale phenomenon like precipitation to look physically realistic. For this, we use Fractal Dimension to gauge spatial intermittency across different quantiles to see if we get it right across all precipitation regimes. LOCA leads with lowest MAE (0.017) with respect to reanalysis owing to its spatial analogue approach which maps regional to local scale patterns. This MAE is followed by δ CLIMBA's MAE (0.021) utilizing a geopositioned encoding attention model to learn spatial patterns while the rest of the methods rely on one-dimensional grid by grid calibration.

One of the biggest concerns from every bias correction method is about preservation of trend between historical and future simulations . Unlike ECDFM and ISIMIP, δ CLIMBA does not include an explicit trend-preservation mechanism, but exhibit better behavior than purely quantile-based methods and LOCA in case of GFDL-ESM4. However this behavior was not repeated again in other GCMs, hence calling for a need for a data-driven mechanism to preserve trends in this framework.

One of the advantages of machine learning based approaches (including differentiable models) is that the trained model is applicable to a completely unseen region or timeframe. Unlike all the traditional methods including LOCA, δ CLIMBA utilizes information from inputs like elevation and landcover to mitigate biases and hence allows it to extrapolate those learned patterns in unseen but similar regions; and results from Figure 8 summarize that the marginal biases like R99pTOT and Rx5day are attenuated with their positive bias distribution moving towards zero. However, the bigger interquartile range and biases exacerbated in indices like SDII and R20 indicate overestimation of precipitation per day limiting the model's reliability to some extent.

There are many directions for future work. The current architecture of δ CLIMBA, though generalizable, is not a universal solution designed to attenuate bias in any GCM, instead it provides a framework to train and tune to our choice of GCM. Extending this framework using a foundational model approach for one-shot bias correction is possibly a better way forward. In addition to that, the spatial encoder could be modified to a more flexible mechanism that could learn long-range spatial dependencies. This improvement may also positively impact performance in spatial tests. Also, an inclusion of statistical or data driven mechanism to better preserve trends could prove beneficial. Finally, this differentiable framework could also be leveraged to understand the mitigation of biases directly by analyzing the coefficients generated from neural networks.

Acknowledgments

This work was supported by U.S. Department of Energy RGCM award DOE DE-SC0016605.

This material is based upon work supported by the National Center for Atmospheric Research, which is a major facility sponsored by the National Science Foundation under Cooperative Agreement No. 1852977.

References

- Aboelyazeed, D., Xu, C., Hoffman, F. M., Liu, J., Jones, A. W., Rackauckas, C., et al. (2023). A differentiable, physics-informed ecosystem modeling and learning framework for large-scale inverse problems: demonstration with photosynthesis simulations. *Biogeosciences*, 20(13), 2671–2692. <https://doi.org/10.5194/bg-20-2671-2023>
- Allard, D., Vrac, M., François, B., & García De Cortázar-Atauri, I. (2025). Assessing multivariate bias corrections of climate simulations on various impact models under climate change. *Hydrology and Earth System Sciences*, 29(18), 4711–4738. <https://doi.org/10.5194/hess-29-4711-2025>
- Bi, D., Dix, M., Marsland, S., O'Farrell, S., Sullivan, A., Bodman, R., et al. (2020). Configuration and spin-up of ACCESS-CM2, the new generation Australian Community Climate and Earth System Simulator Coupled Model. *Journal of Southern Hemisphere Earth Systems Science*, 70(1), 225–251. <https://doi.org/10.1071/ES19040>
- Bindas, T., Tsai, W.-P., Liu, J., Rahmani, F., Feng, D., Bian, Y., et al. (2024). Improving river routing using a differentiable Muskingum-Cunge model and physics-informed machine learning. *Water Resources Research*, 60(1), e2023WR035337. <https://doi.org/10.1029/2023WR035337>
- Boucher, O., Denvil, S., Levavasseur, G., Cozic, A., Caubel, A., Foujols, M.-A., et al. (2018). IPSL IPSL-CM6A-LR model output prepared for CMIP6 CMIP (Version 20250528) [Application/x-netcdf]. Earth System Grid Federation. <https://doi.org/10.22033/ESGF/CMIP6.1534>
- Buser, C. M., Künsch, H. R., Lüthi, D., Wild, M., & Schär, C. (2009). Bayesian multi-model projection of climate: bias assumptions and interannual variability. *Climate Dynamics*, 33(6), 849–868. <https://doi.org/10.1007/s00382-009-0588-6>

- Cannon, A. J., Sobie, S. R., & Murdock, T. Q. (2015). Bias correction of GCM precipitation by quantile mapping: how well do methods preserve changes in quantiles and extremes? *Journal of Climate*, *28*(17), 6938–6959. <https://doi.org/10.1175/JCLI-D-14-00754.1>
- Deser, C., Phillips, A., Bourdette, V., & Teng, H. (2012). Uncertainty in climate change projections: the role of internal variability. *Climate Dynamics*, *38*(3), 527–546. <https://doi.org/10.1007/s00382-010-0977-x>
- Ehret, U., Zehe, E., Wulfmeyer, V., Warrach-Sagi, K., & Liebert, J. (2012). HESS Opinions “Should we apply bias correction to global and regional climate model data?” *Hydrology and Earth System Sciences*, *16*(9), 3391–3404. <https://doi.org/10.5194/hess-16-3391-2012>
- Eyring, V., Bony, S., Meehl, G. A., Senior, C. A., Stevens, B., Stouffer, R. J., & Taylor, K. E. (2016a). Overview of the Coupled Model Intercomparison Project Phase 6 (CMIP6) experimental design and organization. *Geoscientific Model Development*, *9*(5), 1937–1958. <https://doi.org/10.5194/gmd-9-1937-2016>
- Eyring, V., Bony, S., Meehl, G. A., Senior, C. A., Stevens, B., Stouffer, R. J., & Taylor, K. E. (2016b). Overview of the Coupled Model Intercomparison Project Phase 6 (CMIP6) experimental design and organization. *Geoscientific Model Development*, *9*(5), 1937–1958. <https://doi.org/10.5194/gmd-9-1937-2016>
- Feng, D., Fang, K., & Shen, C. (2020). Enhancing streamflow forecast and extracting insights using long-short term memory networks with data integration at continental scales. *Water Resources Research*, *56*(9), e2019WR026793. <https://doi.org/10.1029/2019WR026793>
- Feng, D., Lawson, K., & Shen, C. (2021). Mitigating prediction error of deep learning streamflow models in large data-sparse regions with ensemble modeling and soft data. *Geophysical Research Letters*, *48*(14), e2021GL092999. <https://doi.org/10.1029/2021GL092999>

- Feng, D., Liu, J., Lawson, K., & Shen, C. (2022). Differentiable, learnable, regionalized process-based models with multiphysical outputs can approach state-of-the-art hydrologic prediction accuracy. *Water Resources Research*, *58*(10), e2022WR032404. <https://doi.org/10.1029/2022WR032404>
- Giorgi, F., & Mearns, L. O. (2002). Calculation of average, uncertainty range, and reliability of regional climate changes from AOGCM simulations via the “reliability ensemble averaging” (REA) method. *Journal of Climate*, *15*(10), 1141–1158. [https://doi.org/10.1175/1520-0442\(2002\)015%253C1141:COAURA%253E2.0.CO;2](https://doi.org/10.1175/1520-0442(2002)015%253C1141:COAURA%253E2.0.CO;2)
- Gutjahr, O., Putrasahan, D., Lohmann, K., Jungclaus, J. H., Von Storch, J.-S., Brüggemann, N., et al. (2019). Max Planck Institute Earth System Model (MPI-ESM1.2) for the High-Resolution Model Intercomparison Project (HighResMIP). *Geoscientific Model Development*, *12*(7), 3241–3281. <https://doi.org/10.5194/gmd-12-3241-2019>
- Harder, P., Hernandez-Garcia, A., Ramesh, V., Yang, Q., Sattigeri, P., Szwarcman, D., et al. (2022). Hard-constrained deep learning for climate downscaling (Version 9). arXiv. <https://doi.org/10.48550/ARXIV.2208.05424>
- Hess, P., & Boers, N. (2021, August 25). Deep learning for improving numerical weather prediction of rainfall extremes. <https://doi.org/10.1002/essoar.10507827.1>
- Hess, P., Lange, S., Schötz, C., & Boers, N. (2023). Deep learning for bias-correcting CMIP6-class earth system models. *Earth's Future*, *11*(10), e2023EF004002. <https://doi.org/10.1029/2023EF004002>
- Hochreiter, S., & Schmidhuber, J. (1997). Long Short-Term Memory. *Neural Computation*, *9*(8), 1735–1780. <https://doi.org/10.1162/neco.1997.9.8.1735>
- Hourdin, F., Mauritsen, T., Gettelman, A., Golaz, J.-C., Balaji, V., Duan, Q., et al. (2017). The Art and Science of Climate Model Tuning. *Bulletin of the American Meteorological Society*, *98*(3), 589–602. <https://doi.org/10.1175/BAMS-D-15-00135.1>

- Husain, A., Reddy, J., Bisht, D., & Sajid, M. (2021). Fractal dimension of coastline of Australia. *Scientific Reports*, 11(1), 6304. <https://doi.org/10.1038/s41598-021-85405-0>
- Intergovernmental Panel On Climate Change (Ed.). (2014). Evaluation of Climate Models. In *Climate Change 2013 – The Physical Science Basis* (1st ed., pp. 741–866). Cambridge University Press. <https://doi.org/10.1017/CBO9781107415324.020>
- Intergovernmental Panel On Climate Change (ipcc). (2023). *Climate Change 2021 – The Physical Science Basis: Working Group I Contribution to the Sixth Assessment Report of the Intergovernmental Panel on Climate Change* (1st ed.). Cambridge University Press. <https://doi.org/10.1017/9781009157896>
- Kawai, H., Yukimoto, S., Koshiro, T., Oshima, N., Tanaka, T., Yoshimura, H., & Nagasawa, R. (2019). Significant improvement of cloud representation in the global climate model MRI-ESM2. *Geoscientific Model Development*, 12(7), 2875–2897. <https://doi.org/10.5194/gmd-12-2875-2019>
- Kingma, D. P., & Ba, J. (2017, January 29). Adam: A method for stochastic optimization. arXiv. <https://doi.org/10.48550/arXiv.1412.6980>
- Krasting, J. P., John, J. G., Blanton, C., McHugh, C., Nikonov, S., Radhakrishnan, A., et al. (2018). NOAA-GFDL GFDL-ESM4 model output prepared for CMIP6 CMIP (Version 20250528) [Application/x-netcdf]. Earth System Grid Federation. <https://doi.org/10.22033/ESGF/CMIP6.1407>
- Krinner, G., & Flanner, M. G. (2018). Striking stationarity of large-scale climate model bias patterns under strong climate change. *Proceedings of the National Academy of Sciences*, 115(38), 9462–9466. <https://doi.org/10.1073/pnas.1807912115>
- Lange, S. (2019). Trend-preserving bias adjustment and statistical downscaling with ISIMIP3BASD (v1.0). *Geoscientific Model Development*, 12(7), 3055–3070. <https://doi.org/10.5194/gmd-12-3055-2019>

- LeCun, Y., Boser, B., Denker, J. S., Henderson, D., Howard, R. E., Hubbard, W., & Jackel, L. D. (1989). Backpropagation applied to handwritten zip code recognition. *Neural Computation*, 1(4), 541–551. <https://doi.org/10.1162/neco.1989.1.4.541>
- Li, H., Sheffield, J., & Wood, E. F. (2010). Bias correction of monthly precipitation and temperature fields from Intergovernmental Panel on Climate Change AR4 models using equidistant quantile matching. *Journal of Geophysical Research: Atmospheres*, 115(D10), 2009JD012882. <https://doi.org/10.1029/2009JD012882>
- Li, P., Zha, Y., Shi, L., Tso, C. H. M., Zhang, Y., & Zeng, W. (2020). Comparison of the use of a physical-based model with data assimilation and machine learning methods for simulating soil water dynamics. *Journal of Hydrology*, 584, 124692. <https://doi.org/10.1016/j.jhydrol.2020.124692>
- Li, P., Zha, Y., Zhang, Y., Michael Tso, C.-H., Attinger, S., Samaniego, L., & Peng, J. (2024). Deep learning integrating scale conversion and pedo-transfer function to avoid potential errors in cross-scale transfer. *Water Resources Research*, 60(3), e2023WR035543. <https://doi.org/10.1029/2023WR035543>
- Li, P., Shen, C., Liu, J., Rahmani, F., & Lawson, K. E. (2025, September 22). Structural bias should be addressed before effective parameter learning - Insights from SMAP soil moisture simulations using differentiable process-based models. <https://doi.org/10.22541/essoar.175855507.72741303/v1>
- Livneh, B., Rosenberg, E. A., Lin, C., Nijssen, B., Mishra, V., Andreadis, K. M., et al. (2013). A Long-Term Hydrologically Based Dataset of Land Surface Fluxes and States for the Conterminous United States: Update and Extensions*. *Journal of Climate*, 26(23), 9384–9392. <https://doi.org/10.1175/JCLI-D-12-00508.1>
- Lovejoy, S., Schertzer, D., & Tsonis, A. A. (1987). Functional box-counting and multiple elliptical dimensions in rain. *Science*, 235(4792), 1036–1038. <https://doi.org/10.1126/science.235.4792.1036>

- Maraun, D., Wetterhall, F., Ireson, A. M., Chandler, R. E., Kendon, E. J., Widmann, M., et al. (2010). Precipitation downscaling under climate change: Recent developments to bridge the gap between dynamical models and the end user. *Reviews of Geophysics*, *48*(3), RG3003. <https://doi.org/10.1029/2009RG000314>
- Maraun, Douglas. (2016). Bias correcting climate change simulations - a critical review. *Current Climate Change Reports*, *2*(4), 211–220. <https://doi.org/10.1007/s40641-016-0050-x>
- Maraun, Douglas, Shepherd, T. G., Widmann, M., Zappa, G., Walton, D., Gutiérrez, J. M., et al. (2017). Towards process-informed bias correction of climate change simulations. *Nature Climate Change*, *7*(11), 764–773. <https://doi.org/10.1038/nclimate3418>
- Meisel, L. V., Johnson, M., & Cote, P. J. (1992). Box-counting multifractal analysis. *Physical Review A*, *45*(10), 6989–6996. <https://doi.org/10.1103/PhysRevA.45.6989>
- Mochizuki, T., Tatebe, H., Kataoka, T., & Koyama, H. (2019). MIROC MIROC6 model output prepared for CMIP6 DCP6 (Version 20250527) [Application/x-netcdf]. Earth System Grid Federation. <https://doi.org/10.22033/ESGF/CMIP6.890>
- NASA JPL. (2013). NASA Shuttle Radar Topography Mission Global 1 arc second [Data set]. NASA Land Processes Distributed Active Archive Center. <https://doi.org/10.5067/MEASURES/SRTM/SRTMGL1.003>
- Palmer, T., & Stevens, B. (2019). The scientific challenge of understanding and estimating climate change. *Proceedings of the National Academy of Sciences*, *116*(49), 24390–24395. <https://doi.org/10.1073/pnas.1906691116>
- Pan, B., Anderson, G. J., Goncalves, A., Lucas, D. D., Bonfils, C. J. W., Lee, J., et al. (2021). Learning to correct climate projection biases. *Journal of Advances in Modeling Earth Systems*, *13*(10), e2021MS002509. <https://doi.org/10.1029/2021MS002509>
- Pasos, M. (2020). North American Land Cover, 2020 (Landsat, 30m) [Dataset]. Retrieved March 25, 2026, from <https://www.cec.org/north-american-environmental-atlas/land-cover-30m-2020/>

- Piani, C., Weedon, G. P., Best, M., Gomes, S. M., Viterbo, P., Hagemann, S., & Haerter, J. O. (2010). Statistical bias correction of global simulated daily precipitation and temperature for the application of hydrological models. *Journal of Hydrology*, 395(3–4), 199–215. <https://doi.org/10.1016/j.jhydrol.2010.10.024>
- Pierce, D. W., Cayan, D. R., & Thrasher, B. L. (2014). Statistical downscaling using localized constructed analogs (LOCA)*. *Journal of Hydrometeorology*, 15(6), 2558–2585. <https://doi.org/10.1175/JHM-D-14-0082.1>
- Pierce, D. W., Su, L., Cayan, D. R., Risser, M. D., Livneh, B., & Lettenmaier, D. P. (2021). An extreme-preserving long-term gridded daily precipitation data set for the conterminous United States. *Journal of Hydrometeorology*. <https://doi.org/10.1175/JHM-D-20-0212.1>
- Rahman, M. S., Senkbeil, J. C., & Keellings, D. J. (2023). Spatial and temporal variability of extreme precipitation events in the southeastern United States. *Atmosphere*, 14(8), 1301. <https://doi.org/10.3390/atmos14081301>
- Rahmani, F., Appling, A., Feng, D., Lawson, K., & Shen, C. (2023). Identifying structural priors in a hybrid differentiable model for stream water temperature modeling. *Water Resources Research*, 59(12), e2023WR034420. <https://doi.org/10.1029/2023WR034420>
- Rumelhart, D. E., Hinton, G., & Williams, R. J. (1986). Learning representations by back-propagating errors. *Nature*, 323(6088), 533–536. <https://doi.org/10.1038/323533a0>
- Sawadekar, K., Song, Y., Pan, M., Beck, H., McCrary, R., Ullrich, P., et al. (2025). Improving differentiable hydrologic modeling with interpretable forcing fusion. *Journal of Hydrology*, 659, 133320. <https://doi.org/10.1016/j.jhydrol.2025.133320>
- Shen, C., Appling, A. P., Gentine, P., Bandai, T., Gupta, H., Tartakovsky, A., et al. (2023). Differentiable modelling to unify machine learning and physical models for geosciences. *Nature Reviews Earth & Environment*, 4(8), 552–567. <https://doi.org/10.1038/s43017-023-00450-9>

- Spuler, F. R., Wessel, J. B., Comyn-Platt, E., Varndell, J., & Cagnazzo, C. (2024). ibicus: A new open-source Python package and comprehensive interface for statistical bias adjustment and evaluation in climate modelling (v1.0.1). *Geoscientific Model Development*, 17(3), 1249–1269. <https://doi.org/10.5194/gmd-17-1249-2024>
- Srivastava, A. K., Grotjahn, R., & Ullrich, P. A. (2020). Evaluation of historical CMIP6 model simulations of extreme precipitation over contiguous US regions. *Weather and Climate Extremes*, 29, 100268. <https://doi.org/10.1016/j.wace.2020.100268>
- Tsai, W.-P., Feng, D., Pan, M., Beck, H., Lawson, K., Yang, Y., et al. (2021). From calibration to parameter learning: Harnessing the scaling effects of big data in geoscientific modeling. *Nature Communications*, 12(1), 5988. <https://doi.org/10.1038/s41467-021-26107-z>
- Ullrich, P. (2023). *Validation of LOCA2 and STAR-ESDM Statistically Downscaled Products* (No. LLNL--TR-856094, 2202926, 1085545) (p. LLNL--TR-856094, 2202926, 1085545). <https://doi.org/10.2172/2202926>
- Vano, J., Hamman, J., Gutmann, E., Wood, A., Mizukami, N., Clark, M., et al. (2020). *Comparing Downscaled LOCA and BCSD CMIP5 Climate and Hydrology Projections – Release of Downscaled LOCA CMIP5 Hydrology*. Denver, Colorado: U.S. Department of the Interior, Bureau of Reclamation, with National Center for Atmospheric Research and partners. Retrieved from https://gdo-dcp.llnl.gov/downscaled_cmip_projections/techmemo/LOCA_BCSD_hydrology_tech_memo.pdf
- Vaswani, A., Shazeer, N., Parmar, N., Uszkoreit, J., Jones, L., Gomez, A. N., et al. (2017, December 5). Attention is all you need. arXiv. <https://doi.org/10.48550/arXiv.1706.03762>
- Wang, F., Tian, D., & Carroll, M. (2023). Customized deep learning for precipitation bias correction and downscaling. *Geoscientific Model Development*, 16(2), 535–556. <https://doi.org/10.5194/gmd-16-535-2023>

Wang, L., & Chen, W. (2014). Equiratio cumulative distribution function matching as an improvement to the equidistant approach in bias correction of precipitation. *Atmospheric Science Letters*, 15(1), 1–6. <https://doi.org/10.1002/asl2.454>

Zhou, M. (2016, August 23). Softplus regressions and convex polytopes. arXiv. <https://doi.org/10.48550/arXiv.1608.06383>